PLOS ONE

A transcriptomic analysis of sugarcane response to *Leifsonia xyli* subsp. *xyli* infection

Kai Zhu[1], **Li-Tao Yang**[1], **Cheng-Xi Li**[1], **Prakash Lakshmanan**[2,3,4], **Yong-Xiu Xing**[1]*, **Yang-Rui Li**[1,2]*

1 College of Agriculture, Guangxi University, Nanning, Guangxi, China, **2** Ministry of Agriculture Key Laboratory of Sugarcane Biotechnology and Genetic Improvement (Guangxi), Guangxi Key Laboratory of Sugarcane Genetic Improvement, Sugarcane Research Center, Chinese Academy of Agricultural Sciences, Sugarcane Research Institute, Guangxi Academy of Agricultural Sciences, Nanning, Guangxi, China, **3** Interdisciplinary Center for Agriculture Green Development in Yangtze River Basin, College of Resources and Environment, Southwest University, Chongqing, China, **4** Queensland Alliance for Agriculture and Food Innovation, The University of Queensland, St Lucia, Queensland, Australia

* liyr@gxaas.net (YRL); document126@126.com (YXX)

Abstract

Sugarcane ratoon stunting disease (RSD) caused by *Leifsonia xyli* subsp. *xyli* (*Lxx*) is a common destructive disease that occurs around the world. *Lxx* is an obligate pathogen of sugarcane, and previous studies have reported some physiological responses of RSD-affected sugarcane. However, the molecular understanding of sugarcane response to *Lxx* infection remains unclear. In the present study, transcriptomes of healthy and *Lxx*-infected sugarcane stalks and leaves were studied to gain more insights into the gene activity in sugarcane in response to *Lxx* infection. RNA-Seq analysis of healthy and diseased plants transcriptomes identified 107,750 unigenes. Analysis of these unigenes showed a large number of differentially expressed genes (DEGs) occurring mostly in leaves of infected plants. Sugarcane responds to *Lxx* infection mainly via alteration of metabolic pathways such as photosynthesis, phytohormone biosynthesis, phytohormone action-mediated regulation, and plant-pathogen interactions. It was also found that cell wall defense pathways and protein phosphorylation/dephosphorylation pathways may play important roles in *Lxx* pathogeneis. In *Lxx*-infected plants, significant inhibition in photosynthetic processes through large number of differentially expressed genes involved in energy capture, energy metabolism and chloroplast structure. Also, *Lxx* infection caused down-regulation of gibberellin response through an increased activity of DELLA and down-regulation of GID1 proteins. This alteration in gibberellic acid response combined with the inhibition of photosynthetic processes may account the majority of growth retardation occurring in RSD-affected plants. A number of genes associated with plant-pathogen interactions were also differentially expressed in *Lxx*-infected plants. These include those involved in secondary metabolite biosynthesis, protein phosphorylation/dephosphorylation, cell wall biosynthesis, and phagosomes, implicating an active defense response to *Lxx* infection. Considering the fact that RSD occurs worldwide and a significant cause of sugarcane productivity, a better understanding of *Lxx* resistance-related processes may help develop tools and technologies for producing RSD-resistant sugarcane varieties through conventional and/or molecular breeding.

Introduction

Ratoon stunting disease (RSD) was first discovered in Queensland, Australia in 1945, and occurs in sugarcane growing regions worldwide [1, 2]. RSD infection generally causes 5–30% yield loss, but it can go up to 60% in severely affected ratoon crops [3, 4].

Sugarcane is the most important sugar crop in the world, accounting for about 80% of sugar production globally, and over 90% in China [5, 6]. China is the fourth largest sugar producer in the world. RSD was first reported in China in 1986 [7]. The incidence of RSD in commercial sugarcane crops in China ranges from about 65 to close to 90%, depending on the region [6]. However, it could be significantly higher with recurring and increasingly severe drought.

RSD is a bacterial disease caused by the gram-positive bacteria *Leifsonia xyli* subsp. *xyli* (*Lxx*) [8]. There are no easily distinguishable visual lesions or similar symptoms for RSD. A general growth reduction, decreased stalk diameter and shorter internode length is a common feature of RSD. Because water stress accelerates RSD pathogenesis, the RSD-induced growth reduction is often discounted as drought and/or nutritional deficiency responses, leaving the disease undetected and unchecked. *Leifsonia xyli* subsp. *xyli* is a slow growing and nutritionally fastidious bacterium making it difficult to culture. It takes nearly a month to grow it into a visible colony on solid medium [9, 10]. The predicted *Lxx* pathogenicity genes include those for cellulase, pectinase, wilt-inducing protein, lysozyme, and desaturase, of which the latter is involved in the synthesis of abscisic acid, a hormone that arrests growth [11]. *Lxx* infects its host mainly through wounds on the stalk and is highly infectious. For instance, a previous study showed that diluting the bacteria-containing sap by several hundred-fold still retains strong infectivity [12]. Because *Lxx* mainly inhabits the xylem vessels of sugarcane, RSD has been long recognized as a disease limited to the xylem [13]. Therefore, most of the studies on RSD focused on stem [14–16]. Recent studies using a GFP-labeled *Lxx* strain to track *Lxx* colonization in the whole sugarcane plant found its presence in leaf mesophyll cells as well as those surrounding the vascular bundle sheath [17].

Currently, RSD is mainly controlled by pathogen-free planting material, maintaining good farm hygiene through appropriate field management and strict implementation of quarantine practices [18]. However, some control methods, such as meristem tissue culture are time-consuming and resource-intense, but becoming increasingly popular. Previous studies have shown genotypic variation for resistance to RSD [19]. Nonetheless, breeding for RSD is not a priority in most breeding programs. Hot water treatment, where seedcanes are soaked in hot water maintained at 50°C for two hours is a common method to reduce *Lxx* titre. This method, while economical and practiced widely for commercial cropping, does not completely eliminate *Lxx* [20].

Previous studies have reported reduced water potential and increased membrane permeability and free amino acid levels in sugarcane following *Lxx* infection [21]. *Lxx* infection also affects enzymes involved in plant defenses such as superoxide dismutase (SOD), peroxidase (POD) and catalase (CAT) [16, 22], and alters the level of endogenous plant hormones indole-3-acetic acid (IAA), gibberellic acid (GA) and abscisic acid (ABA) [14, 23]. Further, photosynthesis was found decreased in *Lxx*-infected plants [22, 24]. We observed changes in leaf and stalk anatomy as well as morphological and structural variation in chloroplasts of *Lxx*-infected sugarcane [15, 23]. The genetic elements and mechanisms causing structural and physiological responses of sugarcane to *Lxx* infection are not well understood. Considering the extent of growth and developmental inhibition occurring in *Lxx*-infected sugarcane, it is highly likely that a number of growth- and pathogenicity-related gene networks may be involved in eliciting disease symptoms. Studying global gene expression is an effective and useful approach in

understanding the molecular basis of pathogenesis, and deep transcriptome sequencing technology, RNA-Seq, has been used to investigate disease resistance mechanisms in various plant species [25, 26]. RNA-Seq analysis of rice transcriptome 24 h post-inoculation with blast fungus found up-regulation of 240 genes encoding secreted proteins, including glycosyl, hydrolases and cutinases [27]. RNA-Seq has also been widely used investigate sugarcane abiotic stresses [28, 29], developmental processes such as sugar accumulation [5, 30], self-defoliation [31] and diseases [32–35].

To date studies on RSD have mostly concentrated on developing disease prevention methods [36], diagnostics [37], pathogenesis-related host physiology [14–16, 21–24] and pathogen genome analysis [38]. There is rarely report on global gene expression analysis of healthy and *Lxx*-infected sugarcane. Also, despite sequencing *Lxx* genome, and considerable *Lxx* mutagenesis studies, little is known about the genetic architecture of *Lxx*-sugarcane pathological interactions [11]. RSD pathogenesis-related mechanistic studies are further disadvantaged by the lack of clear and consistent visual disease symptoms other than a generalized growth inhibition of infected plants. With the recent advancements in molecular tools and technology it is now possible to gain insights into molecular aspects of host-pathogen interactions at gene level [33, 39]. The main objective of this study is to identify RSD-associated gene networks and possible reasons for *Lxx*-induced growth inhibition. Also, it is expected that, as with other diseases, comprehensive gene expression analyses will start decoding the RSD host-pathogen interaction black-box and pave the way for future research on molecular targets, including molecular markers, for genetic improvement of sugarcane for RSD resistance. For this study, we used a *Lxx*-susceptible sugarcane variety Badila and conducted RNA-Seq analyses to identify genetic elements and networks associated with RSD pathogenesis in sugarcane.

Materials and methods

Materials and inoculation

Healthy, disease-free seedcanes of sugarcane cultivar Badila (*Saccharum officinarum* L.), which is highly susceptible to RSD, were used for this study. Seedcanes were grown in the greenhouse at the Agricultural College, Guangxi University, Nanning, China. RSD-free status of experimental materials was confirmed by *Lxx* diagnostic PCR assay. The stalk of seedcane plants were cut into single-bud nodal cuttings, called seedcane setts, with sterile knife and immersed in hot water maintained at 50˚C for 2 h to further ensure that they are *Lxx*-free. The *Lxx* strain used for inoculation was *Leifsonia xyli* subsp. *xyli* GXBZ01 (Accession number LFYU00000000). Cultures of this bacterium were prepared as described previously [23]. PCR assay to detect *Lxx* was performed as described elsewhere [21]. The two cut surfaces of seedcane setts were inoculated with 300 μL *Lxx* solution (10^8 cfu/mL). The control group was inoculated with MSC liquid medium. The seedcane setts were kept at 28˚C for two days and then planted in sandy soil. *Lxx*-inoculated and control seedlings at the third-leaf-stage were tested for RSD-infection by PCR assay. The control (*Lxx*-free) and infected plants were then transferred to pots (height × diameter, 350 mm × 300 mm) containing 18 kg of composite soil (soil: sand: organic fertilizer, 6:2:2). Six pots, each carrying three plants, were maintained for each treatment group. At 90 days post-inoculation, top visible dewlap leaf (designated as leaf +1) and basal part of stalk were sampled from three plants selected randomly from the infected and control groups. Collectively there were four groups of samples, each with three biological replicates, totaling 12 biological samples. The four groups of samples were named healthy leaves (HL), healthy stalks (HS), *Lxx*-infected leaves (IL) and *Lxx*-infected stalks (IS), respectively. All the samples were frozen in liquid nitrogen immediately after collection and then stored at -80˚C until used for analyses.

RNA-seq library construction

Healthy and *Lxx*-infected stalks and leaves collected on day 90 post-inoculation were used for high-throughput transcriptome sequencing. Total RNA was extracted using the TRIzol® method [40]. The integrity of the extracted RNA was confirmed using 1% agarose gel electrophoresis. A was used to test the Purity of the extracted RNA was determined by spectrophotometry, using NanoDrop 2000 (Thermo Scientific, Waltham, USA). Fifteen μg of good quality RNA from each sample was used for cDNA library construction. The quality of the cDNA library was determined using an Agilent 2100 Bioanalyzer and ABI StepOnePlus Real-Time PCR system. The cDNA libraries that passed quality assessment were used for sequencing. The cDNA library construction and high-throughput sequencing were conducted at BGI-Shenzhen. An Illumina HiSeq 2000 platform was used for sequencing, employing three biological replicates for every type of tissue used in the experiment.

De novo transcriptome assembly

As the first step, the raw reads were filtered to remove low-quality reads, adaptors, and the reads with high Ns to generate clean reads. From clean reads de novo transcripts were assembled (PCR redundancy was removed to improve the assembly efficiency) using Trinity software [41]. The assembled transcripts were further processed using Tgicl for clustering and redundancy removal and unigenes were generated.

Gene annotation

Unigenes obtained from the assembly were functionally annotated using seven databases; they are KEGG (Kyoto encyclopedia of genes and genomes), GO (Gene ontology), NR (NCBI non-redundant database), NT, Swiss-Prot, Pfam, and KOG (EuKaryotic Orthologous Group) [42].

Analyses of gene expression levels and Differentially Expressed Genes (DEGs)

The clean reads were mapped back to the assembled sequences using Bowtie2 [43], followed by analysis of gene expression level in each sample using RSEM (RNA-Seq by Expectation-Maximization) [44]. Fragments per kilobase of transcript per million mapped reads (FPKM) were used to normalize the gene expression level of every transcript in each sample. The DEGs in sugarcane after *Lxx* infection were identified using edgeR software [45]. The differentially expressed transcripts were selected by applying stringent parameters: i) FPKM > 1, ii) Log_2FC (log_2 fold change) > 1 (up-regulated) or Log_2FC < -1 (down-regulated), iii) p-value < 0.05 and iv) FDR (false discovery rate) < 0.05.

GO and KEGG pathway enrichment analysis

Based on the results of GO and KEGG annotation, as well as official classification, the DEGs were classified (FPKM > = 10: at least one of the three biological replicates of each group of samples had an FPKM > = 10) into groups of cellular function and biological pathway. Meanwhile, R's phyper function was used for GO and KEGG enrichment analysis. The p-values were calculated and subjected to FDR calibration and the functions or pathways showing significant enrichment were identified using a FDR ≤ 0.01.

Real-time quantitative RT-PCR (RT-qPCR)

Reverse transcription quantitative real-time polymerase chain reaction (RT-qPCR) was performed to quantify the expression levels of the transcripts obtained from high-throughput

sequencing. First, TRIzol® (Cowin Biosciences) was used to extract total RNA, followed by RNA quality assessment using NanoDrop 2000. cDNA reverse transcription was performed using a TAKARA PrimeScriptTM RT reagent kit (TaKaRa). RT-qPCR was performed using SYBR Premix Ex Tap^TM II (TaKaRa) using LightCycler®480 II (Roche Applied Science). The PCR reaction mixture and thermal profile were set up as described by Zhu et al. [21]. Gene relative expression levels were calculated using the $2^{-\Delta\Delta Ct}$ method [46]. Primers of candidate genes and an internal reference gene (GAPDH, Glyceraldehyde-3-phosphate dehydrogenase) were designed using Primer 5.0 software and synthesized at Sangon Biotech (Shanghai) Co., Ltd. The primer sequences used are listed in S1 File.

Results

Transcriptome assembly

To study the response of sugarcane to *Lxx* infection at gene level, we performed RNA-Seq of leaf and stalk tissues of *Lxx*-infected and non-infected plants using an Illumina HiSeq 2000 platform with pair-end sequencing technology. After data filtering, 79.73 Gb high-quality clean reads were obtained. De novo assembly of clean reads using Trinity software produced 107,750 unigenes after redundancy removal. The total assembled unigenes contain 165,562,488 nucleotides (approximately 165 Mb), with an average length of 1,536 bp, an N50 value of 2,200 bp, and GC content of 50.73% (Table 1). Within the 107,750 unigenes, 64,135 unigenes (59.52%) were longer than 1,000 bp, among which 11,720 unigenes (10.87%) were longer than 3,000 bp. The distribution of unigenes length is shown in S1 Fig.

Benchmarking Universal Single-Copy Orthologs (BUSCO, https://gitlab.com/ezlab/busco) was used to analyze the assembly results of each sample from 12 groups. It was found that the completeness of all assemblies was > 89%; samples HS-1, HS-2, HS-3, and IS-1 were the best, with > 96% completeness. After removing redundant reads, all samples had a completeness of 97%. Among these, 290 genes were complete, 4 were partially recovered (fragmented) and only 9 were missing (S2 Fig). These results also showed that the de novo assembly of transcripts from the 12 samples covered the majority of sugarcane genes, and the assembly results were suitable for further analyses and experiments.

Transcriptome annotation and analysis of Differentially Expressed Genes (DEGs)

Multiple databases were used to perform functional annotations of the transcripts obtained from the assembly. Among all the databases used, 84,862 transcripts (78.76% of all transcripts)

Table 1. Overview of the assembled sugarcane transcriptome from healthy and *Leifsonia xyli* subsp.*xyli* infected plant tissues.

All-Unigene type	Result
Clean reads (Gb)	79.73
Total Number	107,750
Total Length (bp)	165,562,488
Mean length	1,536
N50 length	2,200
N70 length	1,611
N90 length	839
GC (%)	50.73
TransDecoder identified CDSs	72,733

https://doi.org/10.1371/journal.pone.0245613.t001

were matched to NR, which showed the largest number of matched sequences, followed by KEGG (65,178, 60.49%). In addition, 464,010 (59.41%), 60,914 (56.53%), and 8,709 (45.21%) transcripts were matched to Pfam, Swiss-Prot, and the GO database, respectively ([Fig 1A](#)).

a
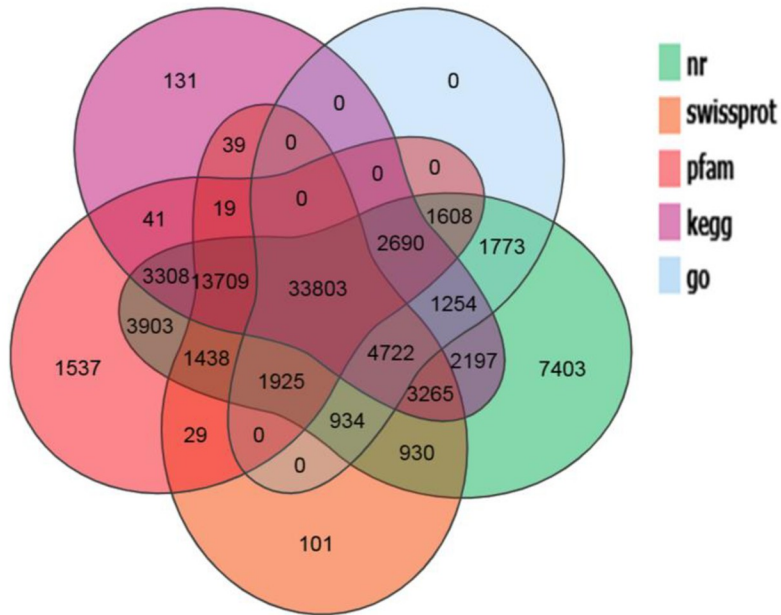
b

Fig 1. Annotation of the assembled sugarcane transcriptome. (a) Venn diagram of genes and predicted proteins aligned to different databases; (b) Distribution of species aligned by the assembled sugarcane genes.

https://doi.org/10.1371/journal.pone.0245613.g001

Fig 2. Heat map of all transcripts of (FPKM>1) (a) sugarcane leaves; (b) sugarcane stalk.

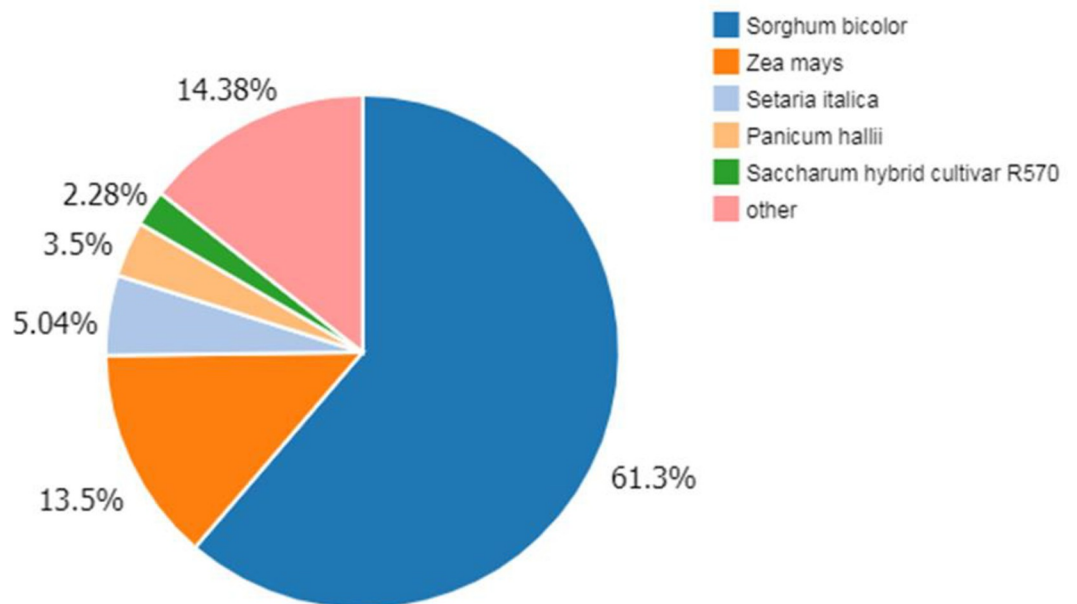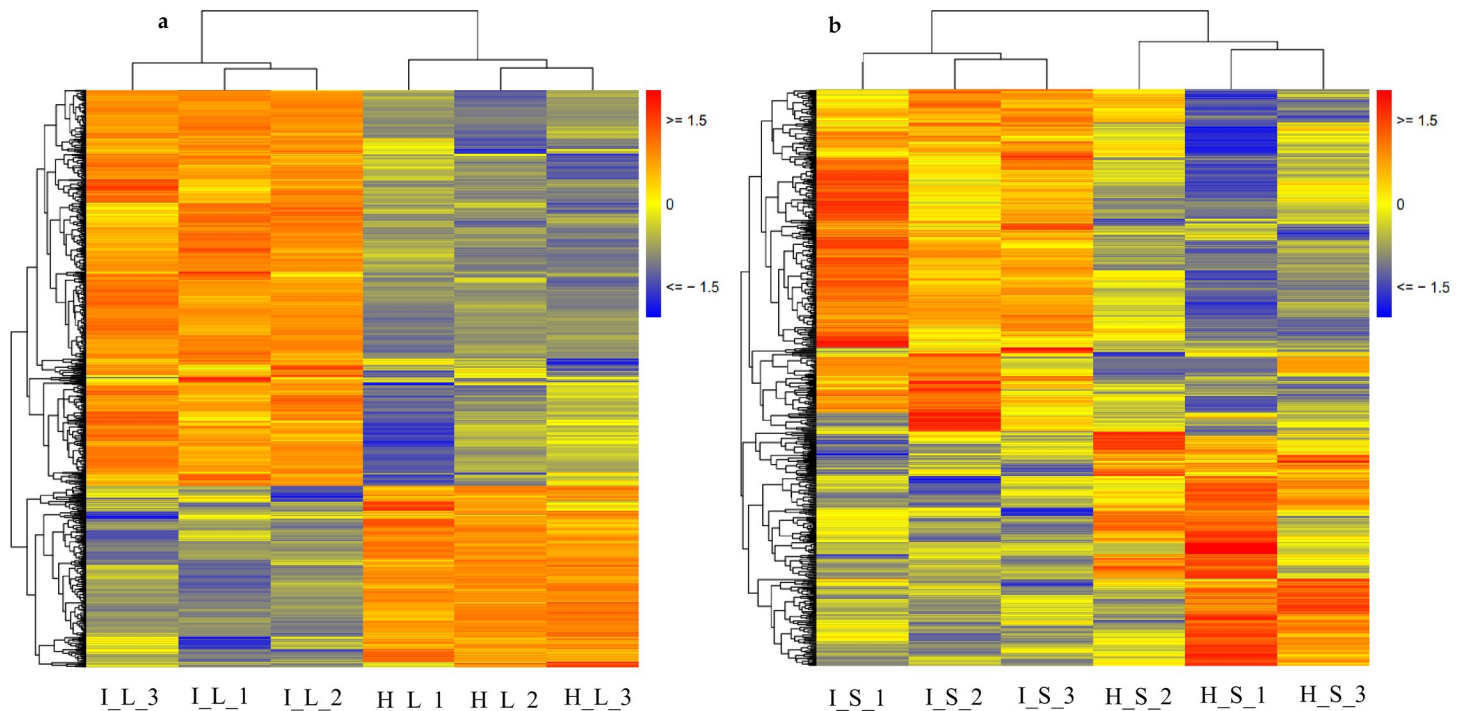Further analysis of NR annotations showed that 52,010 (61.3%) were matched to *Sorghum bicolor*, 11,459 to *Zea mays* (13.5%) and 4,273 to *Setaria italica* (5.04%) (Fig 1B). Of these three species, *S. bicolor* and *Z. mays* are closely related to sugarcane, which further attests the quality and reliability of the assembly.

In the four sample groups, namely, HL, IL, HS, and IS, approximately 77,204 transcripts showed an FPKM≥1, and at least 20% of transcripts in the corresponding sample groups had FPKM≥10 (Fig 2). The distribution of FPKM values was shown in S3 Fig. Pearson correlations for the replicates were above 0.95 in HL, HS, IL, and IS samples (S4 Fig), indicating the reproducibility of replicates. DeSeq software (http://www.bioconductor.org/packages/release/bioc/html/DESeq.html) was used to analyze the differential expression of transcripts among the experimental groups. A large number of DEGs was identified in the *Lxx*-infected leaves (11,802; 7,721 up-regulated and 4,081 down-regulated) and stalks (9,325; 4,266 up-regulated and 5,059 down-regulated), compared to the corresponding tissues from healthy plants. In the leaves, about two-third of the DEGs were up-regulated while in the stalk more DEGs were down-regulated. To identify important DEGs among different groups, we applied filters to obtain DEGs with |Log$_2$FC|≥1, and an average FPKM value≥10.

Functional analysis

Functional analysis was performed to identify the enriched GO terms and KEGG pathways associated with DEGs (FPKM>10) in sugarcane affected by RSD. Among the significant GO terms (Fig 3), 69 genes were involved in "metal ion binding" (GO: 0046872), 12 genes were related to "DNA binding transcription factor activity" (GO: 0003700), and 15 genes were enriched for "peroxidase activity" (GO: 0004601). Next, a bubble plot was used to identify the significant KEGG pathways related to DGEs (Fig 4), and the result showed that 104 DEGs were involved in "RNA transport" (ko03013), which was the most significant
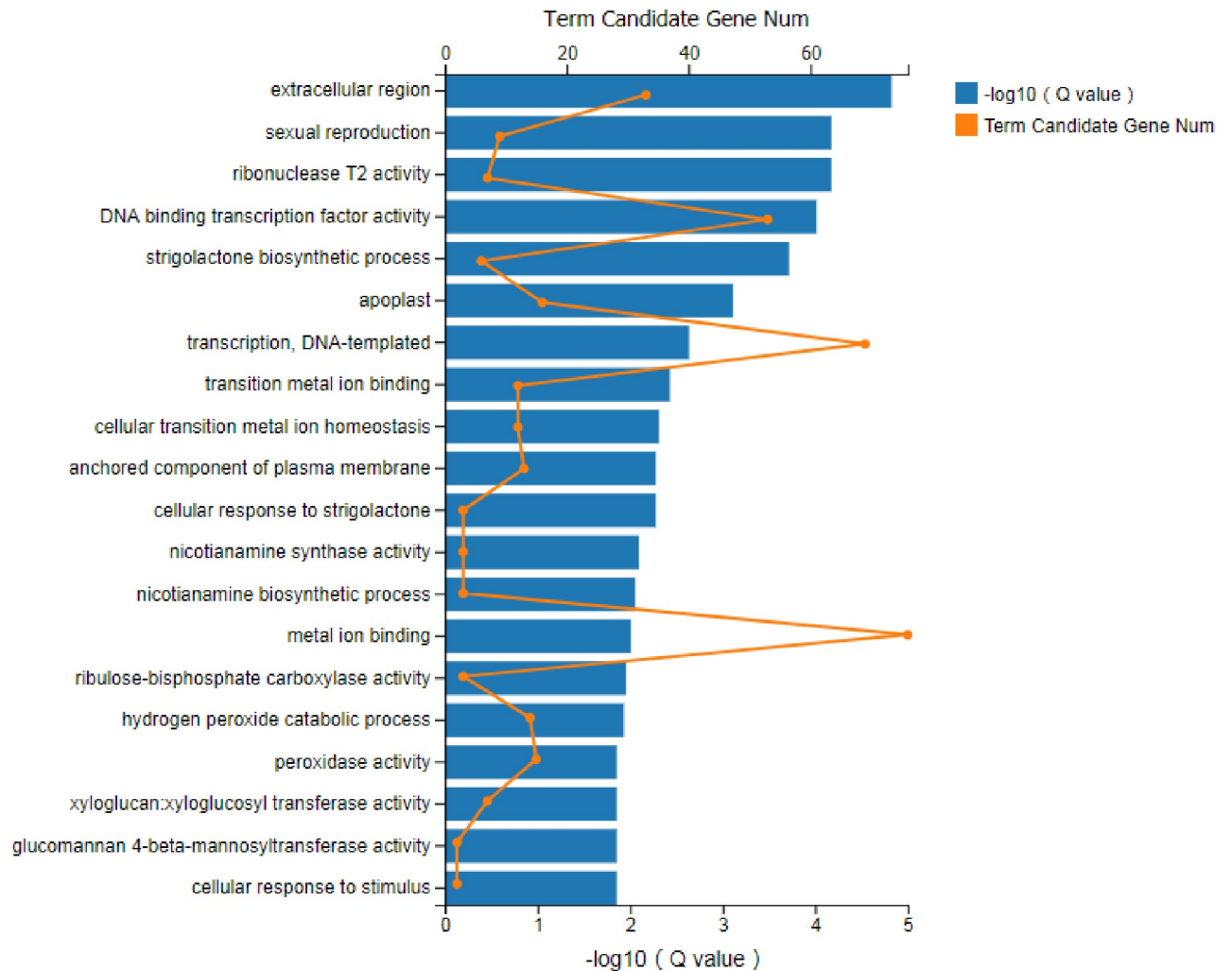
Fig 3. GO enrichment analysis of DEGs (FPKM> = 10) in *Lxx*-infected and healthy sugarcane. The DEGs functions are displayed with respect to their statistical significance (Q value < 0.05). "Term candidate gene num" means the number of genes enriched in each GO term category.

one. Interestingly, 23 DEGs were found involved in "photosynthesis" (ko00195) and "carbon fixation in photosynthetic organisms" (ko00710). Besides, 73 DEGs were found to be involved in the pathways linked to "plant-pathogen interaction" (ko04626). In addition, plant hormone-related pathways such as "flavonoid biosynthesis" (ko00941; 17 DEGs), "diterpenoid biosynthesis" (ko00904; 8 DEGs), "phenylpropanoid biosynthesis" (ko00940; 53 DEGs) and "brassinosteroid biosynthesis" (ko00905; 3 DEGs) were also found to be involved in *Lxx* infection.

Sugarcane genes in response to *Lxx*

The DEGs (FPKM>10) in different functional categories that might be related to sugarcane in response to *Lxx*, such as photosynthesis, phytohormone biosynthesis and metabolism, secondary metabolism related proteins, transcription factors, pathogenesis-related (PR) proteins and some other proteins were analyzed, and the data of these gene families are shown in Fig 5, including the number of genes identified and those involved in various metabolic pathways.
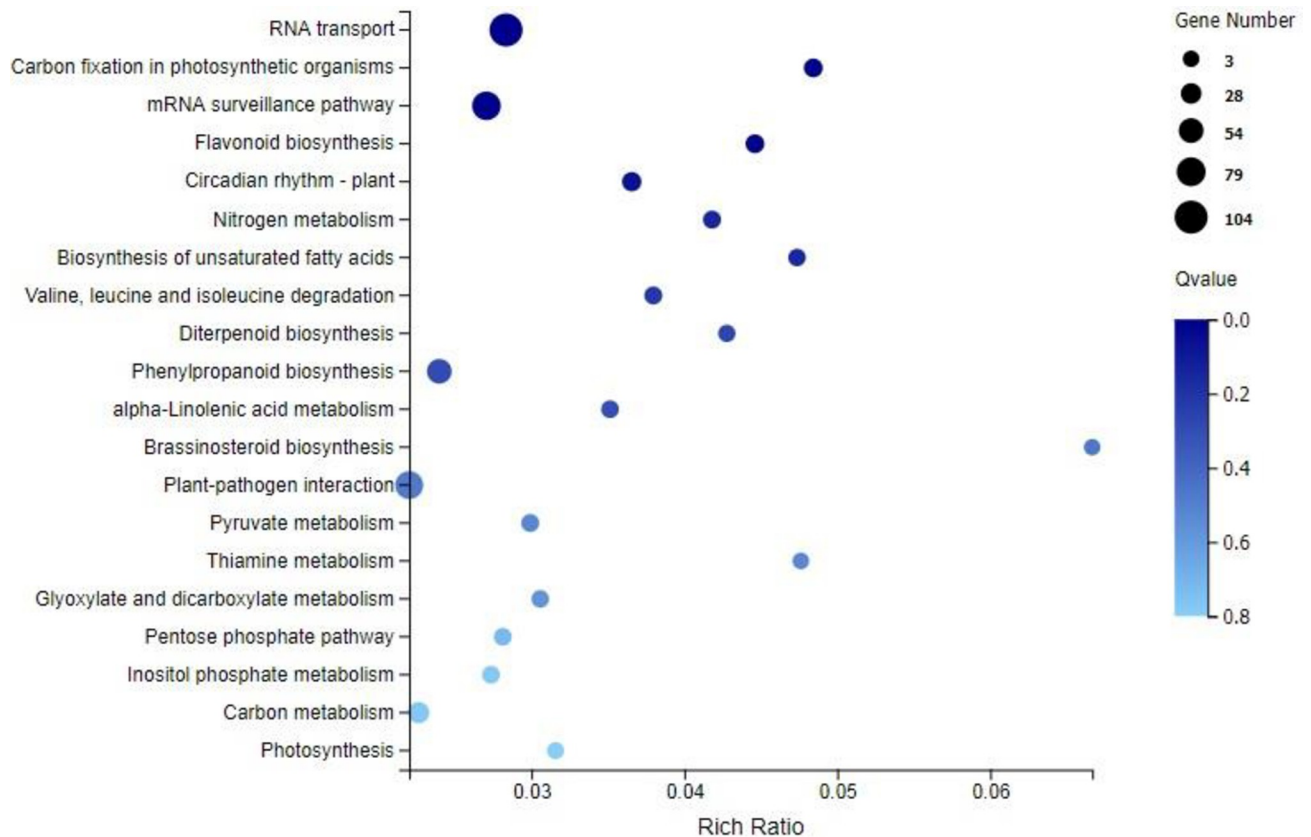
Fig 4. KEGG enrichment analysis of the DEGs (FPKM> = 10) in *Lxx*-infected and healthy sugarcane. Rich Ratio, the ratio of the number of genes annotated to an entry in the selected gene set to the total number of genes annotated to the entry in this species, Rich Ratio = Candidate Gene Num / Gene Num; Bubble size represents the number of genes that are annotated on a KEGG Pathway, color represents enrichment Qvalue, and darker color represents smaller Qvalue lighter color represents higher Qvalue.

https://doi.org/10.1371/journal.pone.0245613.g004

Photosynthesis-related genes. It was found that, with *Lxx* infection, the activity of 51 photosynthesis-related DEGs in leaves (33 up-regulated, 18 down-regulated) and 8 in stalks (5 up-regulated, 3 down-regulated) were altered. However, there were no common photosynthesis-related DEGs present in both leaves and stalks (S2 File; Fig 5). In Ko00195, which is a photosynthesis-related pathway, the genes encoding PSI (*PsaB*, unigene8780), PSII (*PsbH*, unigene1470), F-type ATPase (alpha subunit, CL2043.Contig6), and cytochrome b6-f complex (*PetN*, unigene23696) were all up-regulated, whereas the genes encoding photosynthetic electron transport proteins (*PetH*, CL946.Contig3, and CL946.Contig5) were down-regulated in the leaves. In another pathway related to photosynthesis, Ko00196, the genes encoding antenna proteins (e.g., CL1486.Contig3) were also down-regulated in the leaves. However, these DEGs were not detected in stalks (Fig 5).

Further analysis showed that, out of the 51 DEGs from leaves, 45 were related to chloroplasts (Fig 5). Three chlorophyll-related DEGs were detected in the *Lxx*-infected leaves. Among them, CL1486.Contig3, which was annotated as a light-harvesting protein complex, exhibited down-regulated gene expression. The other two genes, CL5309.Contig2 and unigene8780, however, up-regulated. Following *Lxx* infection, the expression of *RuBP* (Ribulose bisphosphate), a key enzyme in photosynthesis, was down-regulated in the leaves.
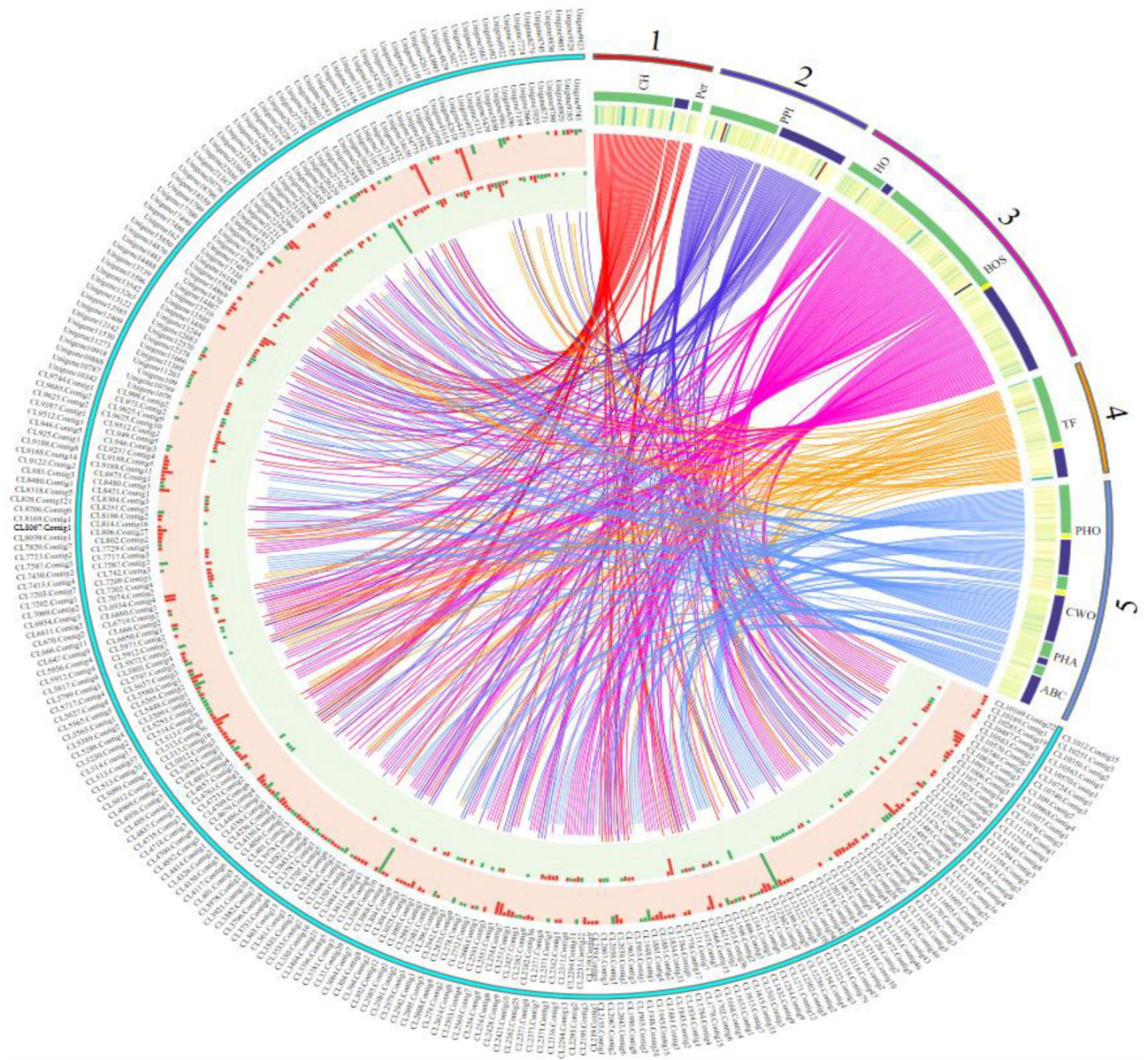
Fig 5. Circular map of crucial genes in response to *Leifsonia xyli* subsp. *xyli*. The inside and outside of the cyan coils represent the gene IDs of DEGs; the corresponding middle circle and the innermost circle represent the gene expression in leaves and stems respectively; the red one represents the up-regulation, and the green one represents the down-regulation. The numbers 1, 2, 3, 4, 5 represent photosynthesis, plant disease interactions, hormone and secondary metabolism, transcription factors, and other genes (genes related phosphorylated, cell walls and ABC transports), respectively. The corresponding green and blue colors represent leaves and stems, respectively.

Signaling pathways in plant-pathogen interactions. In *Lxx*-infected plants, 5% of the total DEGs were found to be involved in the plant-pathogen interaction pathway (KO04626) with 35 and 38 DEGs expressing in the leaves and stalks (S2 File; Fig 5), respectively. No common DEGs between leaves and stalks were detected. Overall, most of the plant-pathogen interactions DEGs encode calcium-dependent protein kinases (CDPKs), pathogenesis-related (PR) proteins, and defense-related TFs. It was found that 48 CDPK-related genes were differentially expressed, with 23 DEGs in the leaves and 25 in the stalks, which comprise 65.75% of DEGs in the plant-pathogen interaction pathway (Ko04626) (S2 File; Fig 5). PR proteins are closely

linked to the induced resistance in plants. Seven DEGs identified were found to be PR proteins in response to *Lxx* infection. Interestingly, most of these DEGs (6) were found in the stalks and down-regulated. In addition, two genes of pathogen-associated molecular patterns (PAMPs) were found in the leaves. It was also found that some *ZFP* (Zinc Finger Protein) and *NBS-LRR* (Nucleotide binding site-leucine-rich repeats) genes, which had been reported as disease resistance genes, were up-regulated in the *Lxx*-infected sugarcane. Besides, heat shock proteins and transcription factors were also found to be involved in the sugarcane-*Lxx* interactions.

Genes related to phytohormone and secondary metabolism. It was found that as many as 167 DEGs in *Lxx*-infected plants were related to phytohormone and secondary metabolism (S2 File). Among these DEGs, 102 genes were from the leaves, 68 from the stalks, and 3 were present in both. In this analysis, 38 DEGs, including 27 in the leaves and 12 in the stalks, are involved in the phytohormone signal transduction pathway (Ko04075). The CL1615.Contig7 gene is particularly interesting because it showed differential expression in both leaves and stalks, but with opposite trends. Its expression was up-regulated 1.27-fold in the leaves and down-regulated 1.05-fold in the stalks (Fig 5). Functional annotation of CL1615.Contig7 indicated that it is a gene encoding SRK2, a Ser/Thr receptor kinase involved in plant development and defense. The DEGs in the phytohormone signal transduction and metabolism pathway (Ko04075) are mainly involved in the biosynthesis of auxin, gibberellin (GA), ethylene (ET), abscisic acid (ABA) and jasmonic acid (JA) (S2 File). Eighteen percent of all the phytohormone-related DEGs identified in response to *Lxx* infection were gibberellin-related and 6 of them were in the leaves and 1 in the stalks (S2 File; Fig 5). The negative regulator of GA signaling, *DELLA* (CL5565.Contig1, CL5565.Contig2, and CL11925.Contig5) [47] was up-regulated, whereas *GID1* (GA-insensitive dwarf 1) (CL1271.Contig6 and CL1271.Contig12) [48] that encodes GA receptors, was down-regulated (Fig 5). Of the other phytohormone-related DEGs, 6 genes were found to encode auxin-related proteins, including auxin responsive factors (ARFs), indoleacetic acid-related proteins (IAAs), and auxin-induced proteins, of which 5 were up-regulated and 1 down-regulated. Among the other phytohormone-related DEGs, 5 genes were related to ET, and all were up-regulated. PYR/PYL, the negative regulators in upstream ABA signal transduction [49], was found up-regulated during *Lxx* infection in sugarcane. It was also found that there were 5 DEGs that were related to JA biosynthesis, among which only one, in the stalk, was up-regulated. In leaves, except for the CL3369.Contig10 gene, which was down-regulated, all the DEGs were up-regulated, including *MYC* (CL9122.Contig2), a central regulator in the JA responsive pathway [50].

In *Lxx*-infected sugarcane, 16 flavonoid-related DEGs were found in the leaves, and two in the stalks; also, 5 phenylalanine-related DEGs were observed in the leaves and one in the stalks (Fig 5). In leaves, the expression of these DEGs was mainly up-regulated. The expressions of *PAL* (CL514.Contig17, CL514.Contig28), *4CL* (CL4056.Contig2, CL12037.Contig4), *CHS* (CL361.Contig1, CL361.Contig6), and *CHI* (CL10487.Contig3, CL11236.Contig1) were all up-regulated in leaves.

Regulation by transcription factors. It was found that the DEGs related to TFs were mainly AP2/EREBP, MYB, WRKY, and MAPK transcription factors (S2 File). In addition, the MADS-box and NAC transcription factors in sugarcane were also differentially expressed in *Lxx*-infected plants. In *Lxx* infected plants 23 AP2/EREBP transcription factor genes were differentially expressed, comprising 37.1% of all transcription factor DEGs found in this study. There were 14 AP2/EREBP transcription factor-encoding DEGs in the leaves, 11 in the stalks, and 2 in the both (unigene2858_All and unigene17492_All). Besides, differential expression of 7 MYBs and 5 WRKY genes were found associated with *Lxx*-infection in sugarcane (S2 File). Analysis showed that upon *Lxx* infection, 6 *MAPK* and 3 *MADS-box* genes were differentially

expressed in the leaves and only 1 each of *MAPK* and *MADS-box* genes in the stalks. The *NAC1* (unigene7159_All) was up-regulated in stalks upon *Lxx* infection.

Other genes involved in *Lxx* stress responses. A total of 36 protein phosphorylation/dephosphorylation genes in sugarcane were differentially expressed in response to *Lxx* infection (S2 File; Fig 5). It was also found that the genes related to phagosomes and lysosomes had altered expression levels (Fig 5). Following *Lxx* infection, many genes involved in cell wall strengthening were upregulated (Fig 5), including 6 cellulose synthase (*CesA*) genes, all of which were found in stalks. In addition, 9 glycosyltransferases (*GTs*) in stalks and 1 GT in the leaves were up-regulated, as well as pectin acetylesterase and polygalacturonate 4-alpha-galacturonosyltransferase (*GAUT1*), both of them are related to pectin biosynthesis. Pectinesterase (*PME*) genes, which are related to pectin degradation, were down-regulated.

RT-qPCR

RT-qPCR was used to validate gene expression in healthy and *Lxx*-infected sugarcane in this study. Nine transcripts were randomly selected for RT-qPCR with three technical replicates. These genes are specifically involved in photosynthesis (Unigene11031_All, Unigene30239_All), plant and pathogen interaction (Unigene10678_All, Unigene41543_All), phytohormones (Unigene7405_All, Unigene115_All), cell walls (Unigene36011_All, Unigene39498_All), and secondary metabolism (Unigene34604_All). The qRT-PCR results (Fig 6) showed similar expression patterns compared to RNA-Seq quantification results. Overall, the up-down expression trend of DEGs was basically consistent both in qRT-PCR and RNA-seq results, indicating the qRT-PCR results support RNA-Seq quantification results.

Discussion

In this study, paired-end sequencing technologies were used to investigate the molecular changes occurring at gene activity level in sugarcane leaves and stalks in response to *Lxx*
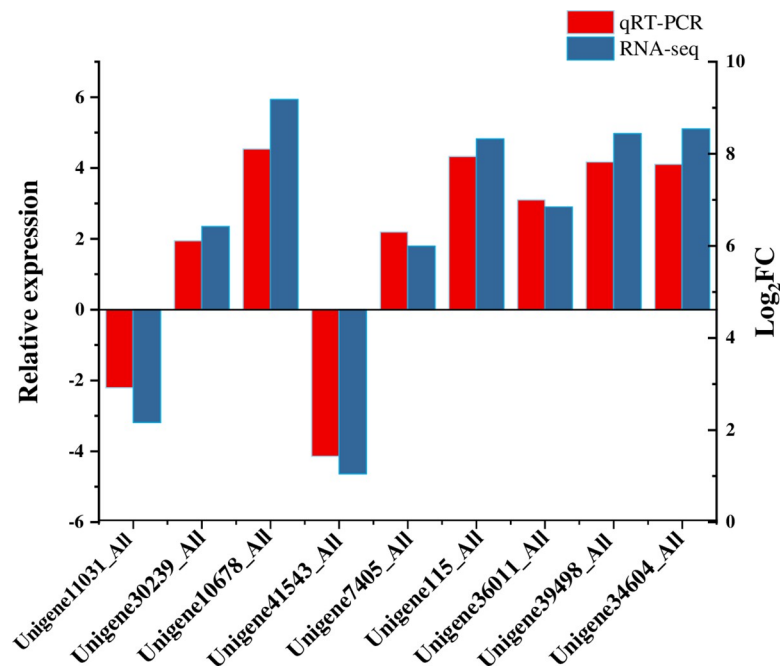

Fig 6. qRT-PCR validation for 9 candidate transcripts. Error bar represents the standard deviation.

infection. This is the first transcriptome study on different RSD-infected sugarcane organs using the deep sequencing technology. Analysis of DEGs (FPKM>10) between HL and IL and between HS and IS has identified 839 DEGs between HL and IL and 610 DEGs between HS and IS with only 21 being common across both comparisons. Stalks and leaves are structurally and functionally very different organs and not surprisingly their gene expression profiles, as shown in this study, are considerably different.

It was found that many DEGs in infected plants are related to sugarcane photosynthesis. Most of the photosynthetic reactions take place in chloroplast, and the number of chloroplast-related DEGs discovered in the diseased plants indicates that *Lxx* infection significantly affected chloroplasts. The majority of these chloroplast-related DEGs were chloroplast membrane genes and *RuBPcase*. The chloroplasts in RSD-infected leaves were deformed, most chloroplasts grana were disappeared, and outer and inner membrane of chloroplasts were deformed [15]. These results [15, 23] are consistent with the down-regulation of chloroplast gene transcription observed in this study. Collectively, these findings suggest that *Lxx* infection severely disrupts chloroplast function, which in turn affects plant growth. Under pathogen stress, antioxidant substances could help maintain the production and availability of adenosine triphosphate (ATP) and nicotinamide adenine dinucleotide phosphate (NADPH) by preserving photosystem function to fix carbon [51]. Upon *Lxx* infection, the genes encoding POD, SOD and CAT were up-regulated, indicating plant's defense to maintain photosynthesis to some extent.

During plant–pathogen interactions, plants trigger a series of defense mechanisms to protect themselves, which include changes in antioxidant enzymes, increase in PR proteins, and phytoalexin biosynthesis [52]. Calcium-dependent Protein Kinases (CDPKs), involved in the regulation of a myriad of growth and developmental process, signal transduction and pathogenesis, exist widely in eukaryotic cells [53, 54]. In this study, the expression of CDPKs was altered considerably, indicating that CDPKs play critical roles in the signaling transduction of defense responses to *Lxx* infection in sugarcane. This was evident from the increased expression of some of the disease resistance genes such as *ZFP* and *NBS-LRR* observed in the present study.

The role of plant hormones salicylic acid (SA), JA, and ET in plant defense responses to pathogens has been extensively studied. Ethylene is involved in regulating plant growth and development, as well as plant responses to biotic and abiotic stresses. Abscisic acid also plays a role in plant-pathogen interactions, mostly as a negative regulator of plant disease-resistance [55, 56]. In this study *PYR* and *PYL* genes, the negative regulators acting upstream in ABA signal transduction [49], were found up-regulated during *Lxx* infection. This is possibly a component of defense strategy operating in sugarcane in response to *Lxx* infection. However, generalized stunting of plant growth is the most prominent visual symptom of RSD and GA is a major regulator of sugarcane growth and development [57]. In *Lxx*-infected sugarcane, up-regulation of *DELLA*, the negative regulator GA response, and down-regulation of *GID1*, which facilitates DELLA protein degradation, were observed. *Lxx* infection-induced inhibition of GA action thus may be a key growth regulatory mechanism in RSD affected plants as observed in other crops infected with different pathogens [58, 59].

Plant secondary metabolites play roles in transducing environmental and biotic stress signals. Many DEGs detected here are involved in the biosynthesis of secondary metabolites, mainly flavonoids and phenylalanine biosynthesis. Phenylalanine is converted into trans-cinnamic acid, catalyzed by L-phenylalanine ammonia-lyase (PAL), which is then converted into 4-hydroxycinnamic acid by cinnamic acid-4-hydroxylase (C4H) and then to 4-coumaroyl-CoA catalyzed by 4-coumaroyl-CoA ligase (4CL), which is used to synthesize alkaloids, lignin, and flavonoids by chalcone synthase (CHS) and chalcone isomerase (CHI) [60]. In this study,

the expression of the *PAL*, *4CL*, *CHS*, and *CHI* genes were upregulated during *Lxx* infection, suggesting that sugarcane responded to *Lxx* infection by increasing the production of polyphenols and other related secondary metabolites with antibacterial properties.

In response to pathogen infection, plants activate numerous transcription factors that are associated with various plant defense strategies such as induced cell death, growth reduction to conserve energy, anatomical modifications and production of antimicrobial agents [61]. Among the major plant transcription factors, APETALA2/ethylene-responsive element binding proteins (AP2/EREBP) form an ancient transcription factor superfamily, of which the AP2 transcription factors regulate reproductive development, while EREBP transcription factors elicit ET and ABA and stress responses [62, 63]. MYB transcription factors are involved in SAR and HR during defense responses [64] while transcription factors WRKY, MAPKs, NAC and MYB were implicated in both biotic and abiotic stress responses and regulation of growth and development [64–69]. In our study, AP2/EREBP, NAC, WRKY, MYB and MAPK showed remarkable differential expression in *Lxx*-infected plants, suggesting the activation of gene networks controlling pathogenesis, disease resistance and growth and development, which tallies well with the growth variation following *Lxx* infection.

Protein phosphorylation serves as a molecular switch in cellular signal transduction and the regulation of enzyme activity [70]. In this study, many DEGs are involved in protein phosphorylation, indicating the large variation in protein phosphorylation/dephosphorylation occurring in *Lxx*-infected sugarcane. For instance, DEGs related to phagosomes and lysosomes were detected, which suggests that sugarcane cells may be defending the infection of *Lxx* through endocytosis. It is well-known that plant cell walls serve as the first physical barrier to pathogen infection. A previous report has characterized the genomic islands in *Lxx* genome that produce pectinase and cellulase involved in cell wall degradation [38] to initiate infection and to channel nutrients from the host. In *Lxx*-infected sugarcane, pectinases and cellulases first degrade the middle lamella and then gradually disintegrate the cell wall. The degraded cell walls with partial deformation produced large amounts of debris that block the pit membrane in host xylem vessels, causing xylem occlusion commonly noticed in RSD-affected sugarcane. This blockage reduces the ability of sugarcane xylem vessels to transport nutrients and water, which exacerbate plant growth inhibition. In our study, many DEGs identified in *Lxx*-infected plants were associated with sugarcane cell wall degradation and this effect was more pronounced in stalks [14].

The molecular mechanism(s) regulating the response to various pathogenic bacterial infections may be similar among different crops as the biological processes underpinning growth and development remain same across plant species. Common response of secondary metabolism was observed in sugarcane during *Acidovorax avenae* subsp. *avenae* [34] and *Colletotrichum falcatum* [35] infection. The activity of genes involved in these two important pathways was also found altered in this study, suggesting the shared molecular response of sugarcane to diverse bacterial pathogenesis.

Conclusion

In conclusion, the present study has considerably advanced the molecular understanding of RSD in sugarcane. Transcriptome sequencing of sugarcane leaves and stalks during *Lxx* infection identified a total of 107,750 unigenes, with nearly 60% of them were longer than 1,000 bp. Gene expression analysis detected 38,513 transcripts representing both RSD-affected and healthy plants studied. Functional analysis revealed that the DEGs are mainly involved in "metabolic pathways", "signal transduction", and "plant–pathogen interactions". *Lxx* infection caused significant variation in transcript abundance associated with chloroplast function. *Lxx* infection inhibited gibberellin response through up-regulation of DELLA and down-regulation of GID1 proteins. The alteration of GA response and the chloroplast-associated gene

expression may account for the majority of growth retardation observed in RSD-affected plants. A number of DEGs were associated with plant-pathogen interactions such as those involved in secondary metabolism, protein phosphorylation/dephosphorylation, cell wall bio-synthesis, and phagosomes, implicating an active defense response to *Lxx* infection. A better understanding of the molecular and physiological basis of RSD pathogenesis-related responses will help develop tools and technologies for producing RSD-resistant sugarcane varieties through conventional and/or molecular breeding.

Supporting information

S1 Fig. Length distribution of the assembled sugarcane transcripts and unigenes.
(PDF)

S2 Fig. Results of transcriptome assembly evaluation results by BUSCO.
(PDF)

S3 Fig. Distribution of normalizedexpression of transcripts detected in all samples.
(PDF)

S4 Fig. Heat map of correlations among replicates based on the gene expression profile.
(PDF)

S1 File. Primers used for RT-qPCR analysis of differentially expressed genes.
(PDF)

S2 File. Differential expression analysis of all genes in *Lxx*-infected compared to healthy sugarcane.
(XLSX)

Acknowledgments

Author Contributions

Conceptualization: Li-Tao Yang, Yang-Rui Li.

Formal analysis: Kai Zhu.

Funding acquisition: Li-Tao Yang, Yang-Rui Li.

Investigation: Kai Zhu, Cheng-Xi Li.

Project administration: Yong-Xiu Xing.

Resources: Yong-Xiu Xing.

Supervision: Li-Tao Yang, Yong-Xiu Xing, Yang-Rui Li.

Writing – original draft: Kai Zhu.

Writing – review & editing: Li-Tao Yang, Prakash Lakshmanan, Yong-Xiu Xing, Yang-Rui Li.

References

1. McDougall WA, Steindl DRL, Elliott JT (1948) Variations in primary vigour in the variety Q.28. Cane Growers' Quarterly Bulletin 12: 31–34.

2. Young AJ (2016) Possible origin of ratoon stunting disease following interspecific hybridization of *Saccharum* species. Plant Pathology 65: 1403–1410.

3. Comstock JC (2008) Sugarcane yield loss due to ratoon stunt. Journal of the American Society of Sugar Cane Technologists 28: 22–31.

4. Grisham MP (1991) Effect of ratoon stunting disease on yield of sugarcane grown in multiple three-year plantings. Phytopathology 81: 337.

5. Chen ZL, Qin CX, Wang M, Liao F, Liao Q, Liu XH, et al (2019) Ethylene-mediated improvement in sucrose accumulation in ripening sugarcane involves increased sink strength. BMC Plant Biology 19: 285. https://doi.org/10.1186/s12870-019-1882-z PMID: 31253103

6. Li YR, Yang LT (2015) Sugarcane agriculture and sugar industry in China. Sugar Tech 17: 1–8.

7. Wu CF, Huang MQ (1986) Ratoon stunting disease in sugarcane was found in mainland China. Sugarcane and Cane Sugar 3: 29–30.

8. Davis MJ, Gillaspie AG, Harris RW, Lawson RH (1980) Ratoon stunting disease of sugarcane: Isolation of the causal bacterium. Science 210: 1365–1367. https://doi.org/10.1126/science.210.4476.1365 PMID: 17817853

9. Brumbley SM, Petrasovits LA, Birch RG, Taylor PW (2002) Transformation and transposon mutagenesis of *Leifsonia xyli* subsp. *xyli*, causal organism of ratoon stunting disease of sugarcane. Molecular Plant Microbe Interact 15: 262–268. https://doi.org/10.1094/MPMI.2002.15.3.262 PMID: 11952129

10. Haapalainen M, Mattinen J, Metzler MC (2000) The growth of a plant-parasitic bacterium, *Clavibacter xyli* subsp. *cynodontis*, is enhanced by xylem fluid components. Physiological and Molecular Plant Pathology 56: 147–155.

11. Brumbley SM, Petrasovits LA, Hermann SR, Croft BJ (2006) Recent advances in the molecular biology of *Leifsonia xyli* subsp. *xyli*, causal organism of ratoon stunting disease. Australasian Plant Pathology 35: 681–689.

12. Comstock JC, Shine JM Jr, Davis MJ, Dean JL (1996) Relationship between resistance to *Clavibacter xyli* subsp. *xyli* colonization in sugarcane and spread of ratoon stunting disease in the field. Plant Disease 80: 704–708.

13. Maramorosch K, Plavsic-Banjac B, Bird J, Liu LJ (1973) Electron microscopy of ratoon stunted sugar cane: Microorganisms in xylem. Journal of Phytopathology 77: 270–273.

14. Chen MH, Huang X, Xie XN, Yang LT, Li YR, Chen BS (2013) Effects of ratoon stunting disease on growth and endogenous hormone in sugarcane. Journal of Huazhong Agricultural University 32: 57–61.

15. Chen MH, Xie XN, Yang LT, Li YR (2013) Effects of ratoon stunting disease on ultrastructural in sugarcane stem cells. Journal of South China Agricultural University 34: 336–339.

16. Xie XN, Zhang XQ, Liang YJ, Yang LT, Li YR (2014) Changes of defense-related enzyme activities in sugarcane under ratoon stunting disease stress. Journal of Southern Agriculture 45: 1551–1557.

17. Quecine MC, Silva TM, Carvalho G, Saito S, Mondin M, Teixeira-Silva NS, et al (2016) A stable *Leifsonia xyli* subsp. *xyli* GFP-tagged strain reveals a new colonization niche in sugarcane tissues. Plant Pathology 65: 154–162.

18. Shen WK, Chen ZH, Yang ZD, Deng HH (2008) Studies on control effect of hot water treatment on sugarcane ratoon stunting disease by and its influence on regenerative plants. Journal of Yunnan Agricultural University 23: 474–478.

19. Croft BJ (2002) A method for rating sugarcane cultivars for resistance to ratoon stunting disease based on an enzyme-linked immunoassay. Australasian Plant Pathology 31: 63–66.

20. Carvalho G, da Silva TGER, Munhoz AT, Monteiro-Vitorello CB, Azevedo RA, Melotto M, et al (2016) Development of a qPCR for *Leifsonia xyli* subsp. *xyli* and quantification of the effects of heat treatment of sugarcane cuttings on *Lxx*. Crop Protection 80: 51–55.

21. Zhu K, Yuan D, Zhang XQ, Yang LT, Li YR (2018) The physiological characteristics and associated gene expression of sugar cane inoculated with *Leifsonia xyli* subsp. *xyli*. Journal of Phytopathology 166: 44–52.

22. Zhang XQ, Liang YJ, Zhu K, Wu CX, Yang LT, Li YR (2017) Influence of inoculation of *Leifsonia xyli* subsp. *xyli* on photosynthetic parameters and activities of defense enzymes in sugarcane. Sugar Tech 19: 394–401.

23. Zhang XQ, Chen MH, Liang YJ, Xing YX, Yang L, Comstock JC, et al (2016) Morphological and physiological responses of sugarcane to *Leifsonia xyli* subsp. *xyli* infection. Plant Disease 100: 2499–2506. https://doi.org/10.1094/PDIS-10-15-1134-RE PMID: 30686166

24. Zhang XQ, Liang YJ, Tang YX, Shao M, Yang LT, Li YR (2015) Morphological characteristic of *Leifsonia xyli* subsp. *xyli* and its effects on photosynthesis of sugarcane. Journal of Huazhong Agricultural University 34: 42–47.

25. Strauß T, van Poecke RMP, Strauß A, Römer P, Minsavage GV, Singh S, et al (2012) RNA-seq pinpoints a *Xanthomonas* TAL-effector activated resistance gene in a large-crop genome. Proceedings of the National Academy of Sciences of the United States of America 109: 19480. https://doi.org/10.1073/pnas.1212415109 PMID: 23132937

26. Zhou X, Bao S, Liu J, Zhuang Y (2016) De Novo sequencing and analysis of the transcriptome of the wild eggplant species *Solanum aculeatissimum* in response to *Verticillium dahliae*. Plant Molecular Biology Reporter 34: 1193–1203.

27. Kawahara Y, Oono Y, Kanamori H, Matsumoto T, Itoh T, Minami E (2012) Simultaneous RNA-seq analysis of a mixed transcriptome of rice and blast fungus interaction. PloS One 7: e49423. https://doi.org/10.1371/journal.pone.0049423 PMID: 23139845

28. Li CN, Nong Q, Solanki MK, Liang Q, Xie JL, Liu XY, et al (2016) Differential expression profiles and pathways of genes in sugarcane leaf at elongation stage in response to drought stress. Scientific Reports 6: 25698. https://doi.org/10.1038/srep25698 PMID: 27170459

29. Liu XH, Zhang RH, Ou HP, Gui YY, Wei JJ, Zhou H, et al (2018) Comprehensive transcriptome analysis reveals genes in response to water deficit in the leaves of *Saccharum narenga* (Nees ex Steud.) hack. BMC Plant Biology 18: 250. https://doi.org/10.1186/s12870-018-1428-9 PMID: 30342477

30. Thirugnanasambandam PP, Mason PJ1, Hoang NV, Furtado A, FBotha FC, Henry RJ (2019) Analysis of the diversity and tissue specificity of sucrose synthase genes in the long read transcriptome of sugarcane. BMC Plant Biology 19: 160. https://doi.org/10.1186/s12870-019-1733-y PMID: 31023213

31. Li M, Liang ZX, He SS, Zeng Y, Jing Y, Fang WK, et al (2017) Genome-wide identification of leaf abscission associated microRNAs in sugarcane (*Saccharum officinarum* L.). BMC Genomics 18: 754. https://doi.org/10.1186/s12864-017-4053-3 PMID: 28946845

32. Ntambo MS, Meng JY, Rott PC, Henry RJ, Zhang HL, Gao SJ (2019) Comparative transcriptome profiling of resistant and susceptible sugarcane cultivars in response to infection by *Xanthomonas albilineans*. Int. J. Mol. Sci. 20: 6138. https://doi.org/10.3390/ijms20246138 PMID: 31817492

33. Huang N, Ling H, Su YC, Liu F, Xu LP, Su WH, et al (2018) Transcriptional analysis identifies major pathways as response components to *Sporisorium scitamineum* stress in sugarcane. Gene 678: 207–218. https://doi.org/10.1016/j.gene.2018.08.043 PMID: 30099025

34. Brigida ABS, Rojas CA, Grativol C, de Armas EM, Entenza JOP, Thiebaut F, et al (2016) Sugarcane transcriptome analysis in response to infection caused by *Acidovorax avenae* subsp *avenae*. PLoS ONE 11: e0166473. https://doi.org/10.1371/journal.pone.0166473 PMID: 27936012

35. Prasanth CN, Viswanathan R, Krishna N, Malathi P, Sundar AR, Tiwari T (2017) Unraveling the genetic complexities in gene set of sugarcane red rot pathogen *Colletotrichum falcatum* through transcriptomic approach. Sugar Tech 19: 604–615.

36. Taylor PWJ, Ryan CC, Birch RG (1988) Harvester transmission of leaf scald and ratoon stunting disease. Sugar Cane 4: 11–14.

37. Taylor PWJ, Petrasovits LA, Van der, Velde R, Birch RG, Croft BJ, Fegan M, et al (2003) Development of PCR-based markers for detection of *Leifsonia xyli* subsp. *xyli* in fibrovascular fluid of infected sugarcane plants. Australasian Plant Pathology 32: 367–375.

38. Monteiro-Vitorello CB, Camargo LEA, Van Sluys MA, Kitajima JP, ruffi D, do Amaral AM, et al (2004) The genome sequence of the gram-positive sugarcane pathogen *Leifsonia xyli* subsp. *xyli*. Molecular Plant-Microbe Interactions 17: 827–836. https://doi.org/10.1094/MPMI.2004.17.8.827 PMID: 15305603

39. Que YX, Su YC, Guo JL, Wu QB, Xu LP (2014) A global view of transcriptome dynamics during *Sporisorium scitamineum* challenge in sugarcane by RNA-Seq. PLoS One 9: e106476. https://doi.org/10.1371/journal.pone.0106476 PMID: 25171065

40. Ji H, Chen M, Greening DW, He W, Rai A, Zhang W, et al (2014) Deep sequencing of RNA from three different extracellular vesicle (EV) subtypes released from the human LIM1863 colon cancer cell line uncovers distinct miRNA-enrichment signatures. PLoS One 9: 110314. https://doi.org/10.1371/journal.pone.0110314 PMID: 25330373

41. Grabherr MG, Haas BJ, Yassour M, Levin JZ, Thompson DA, Amit I, et al (2011) Full-length transcriptome assembly from RNA-Seq data without a reference genome. Nature Biotechnology 29: 644–652. https://doi.org/10.1038/nbt.1883 PMID: 21572440

42. Altschul SF, Madden TL, Schäffer AA, Zhang J, Zhang Z, Miller W, et al (1997) Gapped BLAST and PSI- BLAST: a new generation of protein database search programs. Nucleic Acids Research 5: 3389–3402. https://doi.org/10.1093/nar/25.17.3389 PMID: 9254694

43. Langmead B, Salzberg SL (2012) Fast gapped-read alignment with Bowtie 2. Nature Methods 9: 357–359. https://doi.org/10.1038/nmeth.1923 PMID: 22388286

44. Li B, Dewey CN (2011) RSEM: accurate transcript quantification from RNA-Seq data with or without a reference genome. BMC Bioinformatics 12: 323. https://doi.org/10.1186/1471-2105-12-323 PMID: 21816040

45. Robinson MD, McCarthy DJ, Smyth GK (2010) edgeR: a Bioconductor package for differential expression analysis of digital gene expression data. Bioinformatics 26: 139–140. https://doi.org/10.1093/bioinformatics/btp616 PMID: 19910308

46. Livak KJ, Schmittgen TD (2001) Analysis of relative gene expression data using real-time quantitative PCR and the $2^{-\Delta\Delta Ct}$ Method. Methods 25: 402–408. https://doi.org/10.1006/meth.2001.1262 PMID: 11846609

47. Ubeda-Tomás S, Swarup R, Coates J, Swarup K, Laplaze L, Beemster GTS, et al (2008) Root growth in Arabidopsis requires gibberellin/DELLA signalling in the endodermis. Nature Cell Biology 10: 625–628. https://doi.org/10.1038/ncb1726 PMID: 18425113

48. Murase K, Hirano Y, Sun TP, Hakoshima T (2008) Gibberellin-induced DELLA recognition by the gibberellin receptor GID1. Nature 456:459–463. https://doi.org/10.1038/nature07519 PMID: 19037309

49. Hu S, Wang FZ, Liu ZN, Liu YP, Yu XL (2012) ABA signaling mediated by PYR/PYL/RCAR in plants. Hereditas 34: 560–572. https://doi.org/10.3724/sp.j.1005.2012.00560 PMID: 22659428

50. Shen Q, Xu LU, Zhang L, Gao ED, Tang KX (2012) Advances in the Studies of MYC2 Transcription Factor in Plants. Journal of Shanghai Jiaotong University 30: 51–57.

51. Xu, J.W. Function analysis of Zinc-Finger Protein gene *AtSRZ5* in arabidopsis and proteomic analysis of salt stress treated rice (*Oryza sative* L.) leaves. Ph.D. Dissertation, Nanjing Agricultural University, Nanjing, China, 2014.

52. Hao LM, Wang LA, Ma CH, Yan ZF, Wang JB (2001) Research advances in interaction between pathogenic fungi and plant host. Journal of Hebei Agricultural Sciences 5: 73–78.

53. Hassan A, Okuta T, Kato M, Hatsugai N, Sano Y, Ishimori T, et al (2012) Alternaric acid stimulates phosphorylation of His-tagged RiCDPK2, a calcium-dependent protein kinase in potato plants. Genetics & Molecular Research Gmr 11: 2381–2389. https://doi.org/10.4238/2012.May.10.1 PMID: 22614453

54. Mall TK, Dweikat I, Sato SJ, Neresian N, Xu K, Ge Z, et al (2011) Expression of the rice CDPK-7 in sorghum: molecular and phenotypic analyses. Plant Molecular Biology 75: 467–479. https://doi.org/10.1007/s11103-011-9741-9 PMID: 21318369

55. Cao F, Yoshioka K, Desveaux D (2011) The roles of ABA in plant-pathogen interactions. Journal of Plant Research 124: 489–499. https://doi.org/10.1007/s10265-011-0409-y PMID: 21380629

56. Fan J, Hill L, Crooks C, Doerner P, Lamb C (2009) Abscisic acid has a key role in modulating diverse plant-pathogen interactions. Plant Physiology 150: 1750–1761. https://doi.org/10.1104/pp.109.137943 PMID: 19571312

57. Tavares RG, Lakshmanan P, Peiter E, O'Connell A, Caldana C, Vicentini R, et al (2018) ScGAI is a key regulator of culm development in sugarcane. Journal of Experimental Botany 69: 3823–3837. https://doi.org/10.1093/jxb/ery180 PMID: 29767776

58. Zhu S, Gao F, Cao X, Chen M, Ye G, Wei C, et al (2005) The Rice Dwarf Virus P2 Protein Interacts with ent-Kaurene Oxidases in Vivo, Leading to Reduced Biosynthesis of Gibberellins and Rice Dwarf Symptoms. Plant Physiology 139: 1935–1945. https://doi.org/10.1104/pp.105.072306 PMID: 16299167

59. Martinelli F, Ibanez AM, Reagan RL, Davino S, Dandekar AM (2015) Stress responses in citrus peel: Comparative analysis of host responses to Huanglongbing disease and puffing disorder. Scientia Horticulturae 192: 409–420.

60. Boerjan W, Ralph J, Baucher M (2003) Lignin biosynthesis. Annual review of plant biology 54: 519–546. https://doi.org/10.1146/annurev.arplant.54.031902.134938 PMID: 14503002

61. Jia JH, Wang B (2000) Recent advances in cloning of plant disease resistant gene. China Biotechnology 20: 21–26.

62. Zhao L (2008) Roles of AP2/EREBP family of transcription factors in development and stress response of plants. Chinese Bulletin of Botany 25: 89–101.

63. Zhao SX, Ming C, Lian CL, You ZM (2008) Functions of the ERF transcription factor family in plants. Botany 86: 969–977.

64. Daniel X, Lacomme C, Morel JB, Roby D (1999) A novel myb oncogene homologue in Arabidopsis thaliana related to hypersensitive cell death. The Plant Journal 20: 57–66. https://doi.org/10.1046/j.1365-313x.1999.00578.x PMID: 10571865

65. Luo HL, Chen YH (2011) Advance on transcriptional factors involved in plant disease resistance responses. Journal of Tropical Organisms 2: 83–88.

66. Riechmann JL, Heard J, Martin G, Reuber L, Jiang CZ, Keddie J, et al (2000) Arabidopsis transcription factors: Genome-wide comparative analysis among eukaryotes. Science 290: 2105–2110. https://doi.org/10.1126/science.290.5499.2105 PMID: 11118137

67. Tran LS, Nakashima K, Sakuma Y, Simpson SD, Fujita Y, Maruyama K, et al (2004) Isolation and functional analysis of Arabidopsis stress-inducible NAC transcription factors that bind to a drought-responsive cis-element in the early responsive to dehydration stress 1 promoter. The Plant cell 16: 2481–2498. https://doi.org/10.1105/tpc.104.022699 PMID: 15319476

68. Masaki S (2007) Rice WRKY45 plays a crucial role in benzothiadiazole-inducible blast resistance. The Plant cell 19: 2060–2076.

69. Singh KB, Foley RC, Oñate-Sánchez L (2002) Transcription factors in plant defense and stress responses. Current Opinion in Plant Biology 5: 430–436. https://doi.org/10.1016/s1369-5266(02)00289-3 PMID: 12183182

70. Perazzolli M, Palmieri MC, Matafora V, Bachi A, Pertot I (2016) Phosphoproteomic analysis of induced resistance reveals activation of signal transduction processes by beneficial and pathogenic interaction in grapevine. Journal of plant physiology 195: 59–72. https://doi.org/10.1016/j.jplph.2016.03.007 PMID: 27010348